Analysis and Suppression of EMI for Traction Control Unit Speed Sensors of CRH380BL Electric Multiple Unit

Yutao Tang [1], Feng Zhu [1], Hede Lu [2], and Xin Li [1]

[1] School of Electrical Engineering
Southwest Jiaotong University, Chengdu, 610031, China
835578907@qq.com, zhufeng@swjtu.edu.cn, lxwhere1000@my.swjtu.edu.cn

[2] School of Physical Science and Technology
Southwest Jiaotong University, Chengdu, 610031, China
luhede@qq.com;

Abstract ─ The doors of China railways high-speed 380BL-type (CRH380BL) electric multiple unit (EMU) at Changchun station in China could not be opened. It was analysed that the traction control unit (TCU) speed sensors were disturbed by the pantograph-catenary arc while lowering the pantograph. To solve this problem, firstly, the electromagnetic interference (EMI) for the second train body (02TB) of CRH380BL EMU where the pantograph-catenary is located at is tested. The results show that the intensity of EMI in space is increased significantly because of the pantograph-catenary arc. The distribution of spectrum of EMI is generally random, but the spectrum is mainly distributed in the range from 5MHz to 10MHz. Based on the test results, the coupling mechanism of EMI for the TCU speed sensor is analyzed in this paper. Then a method of nesting magnetic rings on the shielded cable is proposed for suppression of the interference. It can reduce the EMI about 8dB at the main frequency bandwidth mentioned above with 12 centimeters long Ni-Zn ferrite magnetic rings.

Index Terms ─ Electromagnetic interference (EMI), interference suppression, magnetic ring, pantograph-catenary arc, speed sensor.

I. INTRODUCTION

It becomes more and more difficult to ensure EMU in normal operation because of the complex electromagnetic environment [1]. A typical example about that issue is the doors of CRH380BL EMU at Changchun station in China cannot be opened while lowering the pantograph [2-3]. In order to ensure passengers safety, the train doors cannot be opened when the measured speed is beyond 5km/h for this EMU. It is analysed that the TCU speed sensors are disturbed by EMI from the pantograph-catenary arc in above case. Therefore, the further study of EMI for the TCU speed sensors is necessary to ensure reliable operation of EMU.

There are few studies for this issue and most of them mainly focus on speed sensors of China railways high-speed 2-type (CRH2) EMU, such as [4]-[11]. For example, some researchers were concerned about the over voltage caused by conduction interference. However, there were little analysis of the coupling mechanism of interference [4]-[9]. Combined with some experimental investigations, Yang concluded that the damage of sensor under pantograph-catenary detachment was caused by transient train body voltage fluctuation [10]. Zhao said that the surge pulse group would cause faulty speed sensors when the insulation performance of speed sensor became worse [11].

As an extension of previous works, firstly, based on the above description, this paper analyses the working principle of the door control unit (DCU) and the logical relation between TCU speed sensors and DCU of this EMU. Secondly, the EMI of the TCU speed sensor on the second train body (02TB) is tested. The results show that the intensity of EMI in space is increased significantly because of the pantograph-catenary arc. Then the jamming mechanism of the speed sensor is analyzed. Researches show that the common-mode current from the pantograph-catenary arc on the surface of the shield cable causes the instability of the ground potential and lead to above malfunction. A method of nesting magnetic-ring on shield cable of TCU speed sensor to suppress the EMI of common-mode is proposed in this paper. Although there are many researches about using the magnetic-ring to suppress EMI at present [12]-[14], most of them are referring to the simulation model. Few people apply this method to EMI suppression under the above conditions. Experiment is used to verify the effectiveness of suppression in this situation at the end of this paper. It indicates that it can reduce the EMI about 8dB at the main frequency bandwidth mentioned above by using 12 centimeters long Ni-Zn ferrite magnetic rings. The

Submitted On: September 25, 2017
Accepted On: April 16, 2018

method is also effective for discrete interference in 10MHz~30MHz.

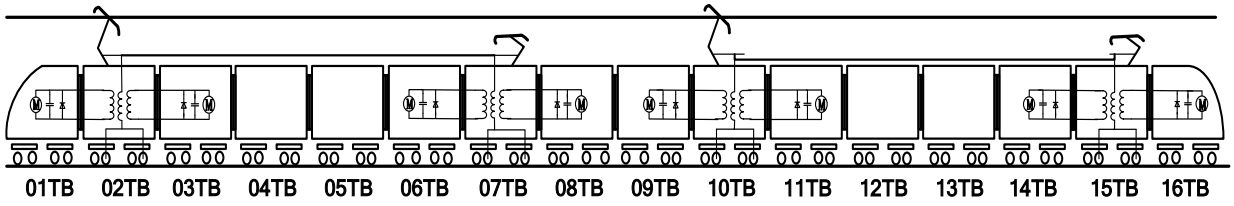

Fig. 1. Structure for the TBs of CRH380BL EMU.

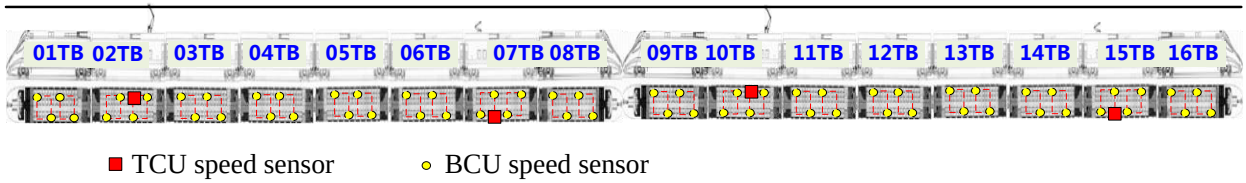

Fig. 2. Diagram of speed sensors position distribution in CRH380BL EMU.

II. ANALYSIS OF LOGICAL RELATIONSHIP FOR TRAIN DOORS

As for the TBs of CRH380BL EMU, the Fig. 1 shows its structure, consisting of 16 marshaling TBs. Their serial numbers are from 01 to 16. The motors are 01TB, 03TB, 06TB, 08TB, 09TB, 011TB, 14TB and 16TB, and all the remaining of TBs are trailers. Besides, there are four pantographs on the train roofs of 02TB, 07TB, 10TB and 15TB respectively. The rest of two pantographs are in standby when the pantographs on the train roofs of 02TB and 07TB being used and vice versa.

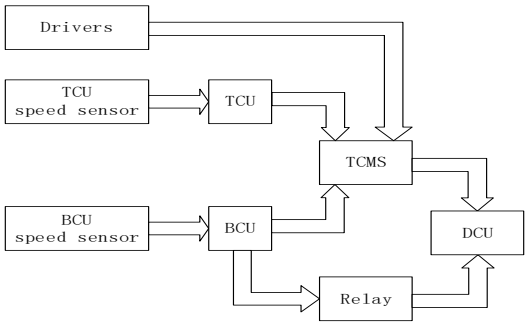

Fig. 3. The logic diagram of DCU.

There are two types of speed sensors on the CRH380BL EMU: TCU speed sensors and brake control unit (BCU) speed sensors. The installation position of those sensors is shown in Fig. 2. According to the CRH380BL EMU, the closure of door is controlled by the DCU. As described in Fig. 3, there are three ways to close the train doors. First of all, the driver can send message to DCU directly to close all the doors by train control and management system (TCMS). Secondly, the two kinds of speed sensors send the speed signal into TCU and BCU respectively, and the signal will be compared with 5km/h. As long as the speed is measured by one of TCU speed sensors is more than 5km/h, all the doors will be closed. As for the BCU speed sensors, it can only give the control to the corresponding train doors. For example, if the speed is detected by one of BCU speed sensors on 02TB exceeds the limit, then just the train door of 02TB won't be opened. Thirdly, when a speed signal which is detected by the BCU speed sensors is far greater than 5km/h, the signal will be sent to DCU by the relay instead of TCMS to close the door quickly.

III. EMI TEST

A. The magnetic field test

The pantograph-catenary arc will be formed between the catenary and the pantograph when the EMU is lowering the pantograph. Its main frequency component is about 5MHz [15], and it can generate the powerful magnetic field. A CRH380BL EMU which had above fault was selected as a test object at Changchun station in China. The strength of the magnetic field in the space was tested by using the EMI receiver (ESCI-3; 9KHz~3GHz; -40dBμV~+137dBμV) and the loop antenna (HFH2-Z2; 9KHz~30MHz). The situation of field test is shown in Fig. 4.

Taking 02TB as the object of study, the magnetic field intensity was measured several times when the pantograph of 02TB being lowered. The loop antenna was erected at a horizontal distance of 3m from the center of the orbit. The maximum magnetic field intensity could be close to 54dBμA/m (The antenna coefficient of the loop antenna is 20dB/m within the frequency range of this test). Some electromagnetic sensitive devices can be disturbed by such high frequency and large amplitude magnetic field. However, the magnetic field intensity

will be reduced significantly when it is far away from the pantograph. Because the CRH380BL EMU is about 400 meters, the speed sensors which is far away from 02TB won't be influenced when the pantograph of 02TB being lowered.

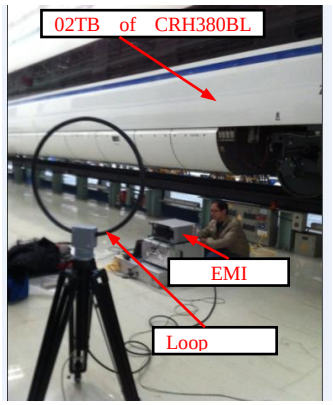

Fig. 4. The field test of magnetic field intensity.

According to the working principles of speed sensors and the DCU, the BCU speed sensors just affect the corresponding doors and the TCU speed sensors can influence all the doors of this EMU. All the doors instead of the single door could not be opened normally in this fault. We believe that TCU speed sensor was disturbed and led to this breakdown.

B. The EMI test of TCU speed sensor

The EMI of TCU speed sensor on 02TB was tested by using the spectrum analyzer (Agilent 9340B; 9KHz~3GHz; -40dBμV~+137dBμV) and current clamp (BK-CP-02; 10Hz~100MHz) when the pantograph of 02TB being lowered. The situation of physical connections is shown in Fig. 5. The Fig. 6 shows the test results without lowering the pantograph. It comes from the electromagnetic waves that already exist in the environment. The two typical results of test are displayed in Fig. 7.

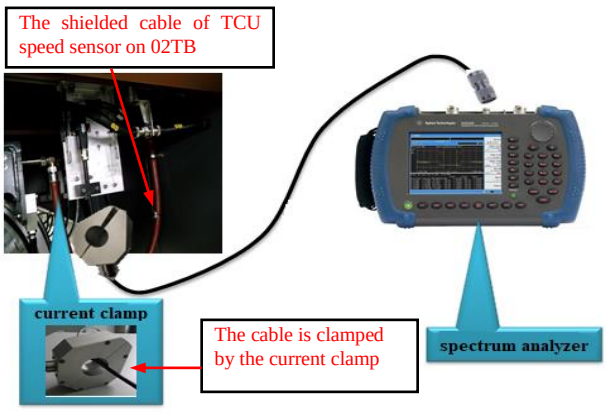

Fig. 5. The diagram of physical connections.

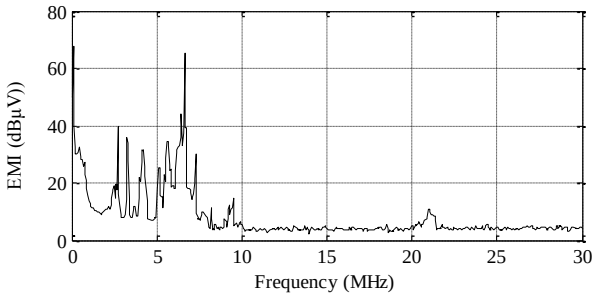

Fig. 6. The test results without lowering the pantograph.

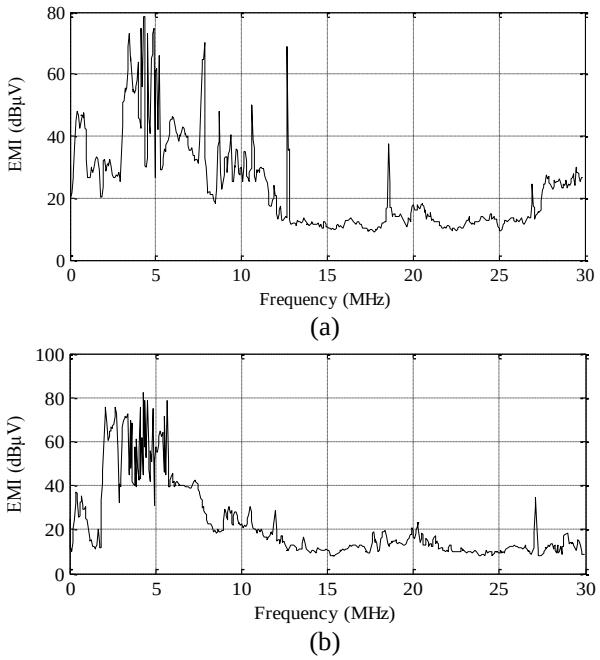

Fig. 7. The waveform of EMI for TCU speed sensor.

The results show that the pantograph-catenary arc will cause EMI on the cable of the speed sensor. The distribution of spectrum of EMI is generally random, but the spectrum is mainly distributed in the range from 5MHz to 10MHz. A small amount of discrete interference occur in the range of 10MHz~30MHz.

IV. ANALYSIS OF THE MECHANISM OF EMI

There is a high frequency component in the pulse wave which is emitted by the pantograph-catenary arc. It can cause the disturbance on the shield cable of speed sensors. The outer conductor of the cable braid shield of TCU speed sensor is made of metal wire. As described in Fig. 8, the cable braid shield is not shielded completely because of the many tiny holes on it. The induced electric field *E* will be formed on the surface of the cable because of the EMI. A portion of the interference will be coupled to the core wire inside the cable through

tiny holes. It can form the induced electric field *E*' on the core wire as depicted in Fig. 9. Because the *E*>*E*', it will form a potential difference *U* between the cable braid shield and core wire. The value of interference can be expressed by the value of *U* [16]:

$$U = I \times Z_t \times L_m, \quad (1)$$

where I is the induced current, Z_t is the transfer impedance of each meter cable, L_m is the effective length of the cable. Based on document [17], Z_t is given by:

$$Z_t = Z_d + j\omega(M_h \pm M_b), \quad (2)$$

where Z_d is the diffusion impedance, its value decreases as the increase of frequency [18]:

$$Z_d \approx \frac{4}{\pi d^2 nC\sigma\cos\alpha} \cdot \frac{(1+j)d/\delta}{\sinh[(1+j)d/\delta]}, \quad (3)$$

M_h is the hole inductance and M_b is the braid inductance [19]:

$$M_h = \frac{2\mu_0 C}{\pi\cos\alpha}\left[\frac{b}{\pi(d_0+2d+h)}\right]^2 \exp(-\frac{\pi d}{b}-2\alpha), \quad (4)$$

$$M_b = \frac{\mu_0[ndh+(b-\frac{bh}{d})\frac{h+d}{2}+B]A}{2\pi C(d_0+2d+h)\cos\alpha}, \quad (5)$$

where d is the wire diameter, C is the number of carriers in the braid, n is the number of wires in each carrier, δ is the skin depth, σ is the conductivity of shield and b is the distance between the adjacent carriers. The value of the pitch angle of the weave α and the distance between the braid layers h can be calculated accurately by using the picks p (number of carrier crossings per unit length) and the diameter under the braid d_0 [20],
and

$$A = (\sqrt{v}+1)^2\cos(2\alpha), \quad (6)$$

$$B = n(d^2 - \frac{\pi d^2}{4}). \quad (7)$$

Where v is the number of holes in the braid.

The type of braided coaxial cables which are used on TCU speed sensors of the CRH380BL EMU are determined by the following primary parameters: d=0.12mm, C=24, n=6, d_0=5.54mm, p=45mm, σ=5.8×107S/m, μ_0=4π×10-7H/m. As shown in Fig. 10, the calculated values Z_t by the formula (2)~(7) are higher than the test values generally, especially at the high frequency band. Therefore, it is necessary to revise the formula for the calculation of Z_t.

Because the response of the high frequency transient electromagnetic field on the woven mesh is more complex. The extra attenuation of vortex current caused by the magnetic field between the inner and outer layers of the braid network cannot be ignored. Therefore, the extra fluctuating effects M_e [21] is added into the calculation of Z_t:

$$M_e = -\frac{1.16}{Cnd}\arctan\frac{n}{3}\sin(\frac{\pi}{2}-2\alpha)\sqrt{\frac{\mu_0}{\sigma}}\sqrt{\omega}e^{j\frac{\pi}{4}}. \quad (8)$$

At the same time, the attenuation of transmitted electromagnetic waves at high frequency will not be ignored when the woven mesh with curvature. Therefore, the curvature coefficient K of woven mesh is proposed to revise the M_h in this study, and the values of K are from 0 to 1. The Fig. 11 shows the variation of the transfer impedance (M_e has been added) of the above cable with several typical values of K.

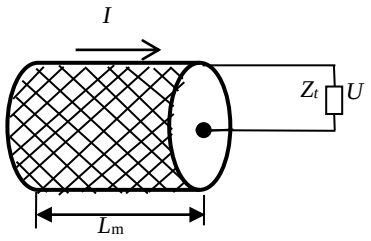

Fig. 8. The diagram of braided coaxial cable.

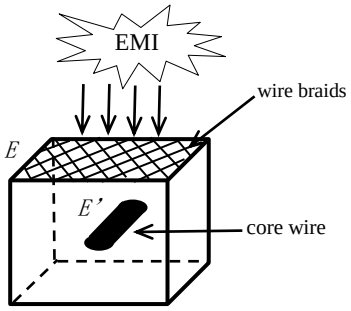

Fig. 9. The section of braided coaxial cable.

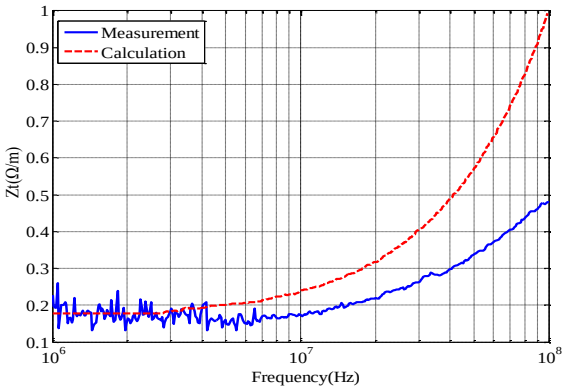

Fig. 10. The comparative diagram of the calculated values and the test values of Z_t.

The results of calculation and measurement of transfer impedance with different K are compared in large quantities. The calculated values of Z_t for this cable is the closest to the test values when the K is 0.85

within the frequency range of 30MHz. So formula (4) has been amended:

$$M_h^* = 0.85 M_h . \quad (9)$$

The formula (2) has been modified:

$$Z_t^* = Z_d + j\omega(M_h^* \pm M_b) + M_e . \quad (10)$$

The comparison of the calculated values of Z_t^* and the test results is shown in Fig. 12.

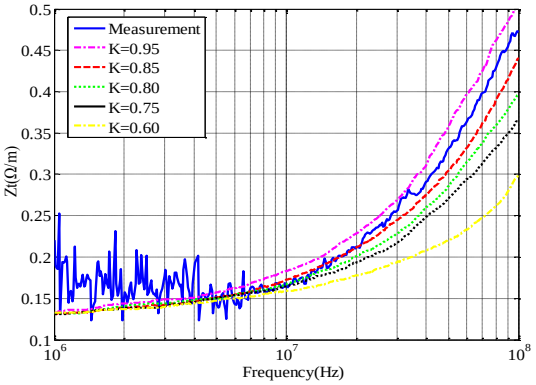

Fig. 11. The curve of the values of the transfer impedance with different *K*.

The values of I and L_m are got by field test. The maximum value of I on the shield cable is 95mA. The L_m of TCU speed sensor on 02TB is 1m. The rest of shield cable is inside the metal housing, and it will not be disturbed. The Fig. 7 shows that the EMI is mainly concentrated in the frequency range of 5MHz~10MHz. Z_t^*=150mΩ/m can be calculated when f=5MHz (The EMI of the pantograph-catenary arc is random. But the frequency of the strongest interference is about 5MHz by field test). The U can be calculated: U≈14mV.

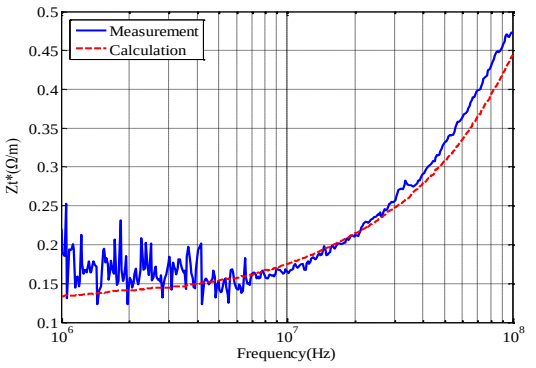

Fig. 12. The comparative diagram of the calculated values and the test values of Z_t^*.

According to the test results shown in Fig. 7, the maximum interference of TCU speed sensor on 02TB is about 80dBμV. The voltage value can be converted to 10mV, which is consistent with the theoretical analysis.

The above voltage is calculated at single frequency point. The actual interference voltage will reach up to about 4kV because of the superposition of power energy spectrum [22]. It was the instantaneous high voltage that led to the fault of speed sensors.

V. TEST RESULTS OF INTERFERENCE SUPPRESSION

The method of nesting Ni-Zn ferrite magnetic rings on shield cable of TCU speed sensor is used to suppress EMI in this paper. Ni-Zn ferrite magnetic rings are often used to suppress 1MHz or more high-frequency EMI because of its low permeability and high resistivity [23].

The interference suppression characteristics of four different Ni-Zn ferrite magnetic rings are compared in Table 1. Their sizes are suitable for the cables of the TCU speed sensors and the impedance-frequency curve are shown in Fig. 13. It can be seen that the interference suppression capability of type 1 is the strongest in the main frequency mentioned above (5MHz~10MHz) of EMI. As a result, type 1 (E04SR401938) is chose in this study.

In order to study the suppression of the EMI by magnetic rings, a simulation experiment has been done in the laboratory. The sinusoidal signal generated by the signal generator (Agilent N9310A; 9KHz~3GHz; -127dBm~+13dBm) was radiated by the transmitting antenna (HK116; 30MHz~1GHz) onto the cable (Length is 1m) of the TCU speed sensor. The spectrum analyzer, current clamp and loop antenna mentioned above were used to receive interference on the cable. The suppression effect of EMI after nesting the Ni-Zn ferrite magnetic rings (type 1) with different numbers on cable was tested, and the results were shown in Fig. 14.

Table 1: The main parameters of four different types of magnetic rings

Type	Part No.	Internal Diameter	External Diameter	Height
1	E04SR40 1938	19mm	38mm	40mm
2	E04ST25 1512D	15mm	28mm	12mm
3	E04ST28 1613D	16mm	31mm	13mm
4	E04ST40 2715D	27mm	42mm	15mm

Because the height of magnetic ring (type1) is 40mm and the length of cable is 1m, it results that the maximum number of that rings is 25. As shown in Fig. 14, the suppression effect is not increased obviously when the number of magnetic rings is increased to more than 5. According to the results of the experiment, the different numbers of magnetic rings (type1) are nested on the cable of TCU speed sensor on 02TB of this EMU.

When the number of the magnetic rings is greater than three, that is, when the suppression effect is more than 8dB, the malfunction of the abnormal locking for the train doors can be solved.

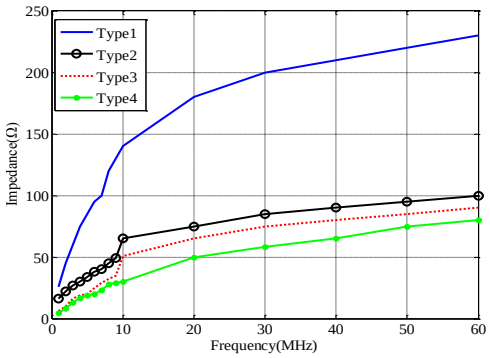

Fig. 13. The impedance-frequency curve of four Ni-Zn ferrite magnetic rings.

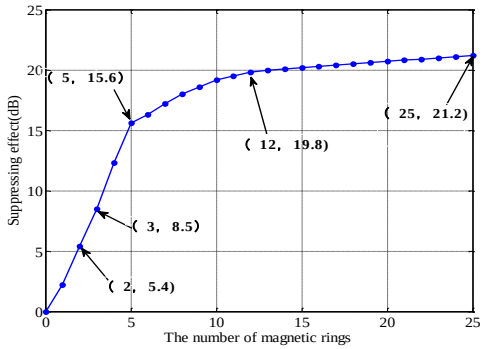

Fig. 14. The suppression effect of EMI after nesting different numbers of magnetic rings on cable.

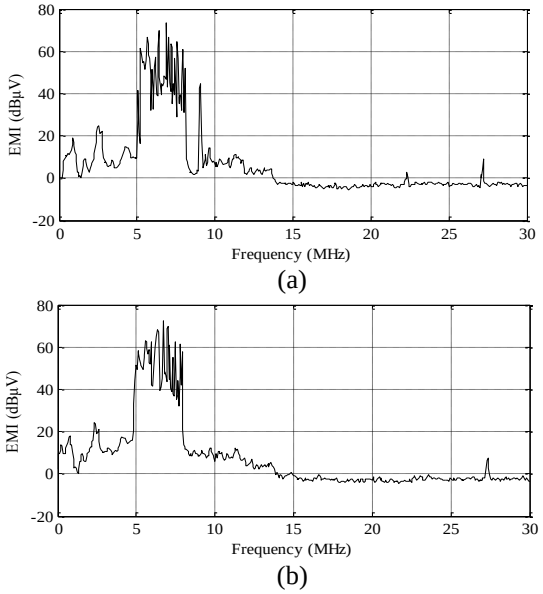

Fig. 15. The waveform after EMI is suppressed.

When the pantograph of 02TB being lowered, the EMI was tested after nesting three Ni-Zn ferrite magnetic rings on the shield cable of TCU speed sensor on 02TB. The results are shown in Fig. 15.

As shown in Fig. 15, the peak of EMI is decreased by about 8dB after using the magnetic ring when the frequency is below 10MHz. When the frequency is 10MHz~30MHz, the discrete interference is reduced obviously. Basically, the magnetic rings can absorb the electromagnetic radiation energy and reduce Z_t of cable. So as to achieve the purpose of interference suppression. In this way, the train doors can be opened normally.

VI. CONCLUSION

In this paper, a method of suppressing the EMI from the pantograph-catenary arc for the TCU speed sensor of CRH380BL EMU was proposed. Based on the malfunction of this EMU at Changchun station in China, the mechanism of EMI was analyzed systematically. It indicated that the TCU speed sensors were disturbed and led to the fault of DCU. According to the test results, the abnormal locking of the train doors was solved effectively after nesting three (12cm) Ni-Zn ferrite magnetic rings on the shield cable of TCU speed sensor.

ACKNOWLEDGMENT

We would like to thank the anonymous reviewers for their insightful comments. This paper is supported by the National Natural Science Foundation of China (U1434203).

REFERENCES

[1] F. Zhu, D. P. Niu, and C. W. Xu, "Measurement and analysis on ambient magnetic field inside the bodywork of CRH1," *Journal of Electric Science and Technology*, vol. 27, no. 2, pp. 42-46, June 2012.

[2] K. Huang, Z. G. Liu, F. Zhu, Z. S. Zheng, and Y. Cheng, "Evaluation scheme for EMI of train body voltage fluctuation on the BCU speed sensor measurement," *IEEE Transactions on Instrumentation and Measurement*, vol. 66, no. 5, pp. 1046-1057, May 2017.

[3] J. B. Yang, F. Zhu, J. Li, M. Sha, and D. Q. Yuan, "Electromagnetic interference measurement and analysis of high-speed electric multiple units speed sensor," *Journal of Electronic Measurement and Instrumentation*, vol. 29, no. 3, pp. 433-438, Mar. 2015.

[4] G. Gao, B. Yuan, Y. Feng, and G. Wu, "Over-voltage analyzing for high speed railway phase-separation switch," *in Proc. International Conference on Electric Power Equipment - Switching Technology IEEE*, pp. 207-209, 2012.

[5] H. Wu, "Research on Vehicle Body Over-Voltage Surge," Department of Electrical Engineering,

Southwest Jiaotong University, M.S., 2013.
[6] S. Hatsukade, "Reduction method of surge voltage on AC railcar's body," *Foreign Rolling Stock*, vol. 50, no. 2, pp. 70-75, 2010.
[7] S. Hatsukade and M. Nagata, "Reduction of EMI from traction circuits using shielded cable," *Qr of Rtri*, vol. 49, no. 1, pp. 20-25, Feb. 2008.
[8] S. Hatsukade and T. Maeda, "Experiment and basic analysis of the surge on a rolling stock's body," *IEEE Trans. P&E*, vol. 125, no. 8, pp. 754-758, 2005.
[9] W. F. Han, X. Y. Hu, S. Xiao, G. N. Wu, G. Q. Gao, D. L. Liu, and K. S. Yang, "Analysis of railcar's body over-voltage for electric multiple unit in the case of lightning contact," *Journal of Railway Science & Engineering*, vol. 10, no. 4, pp. 117-123, Aug. 2013.
[10] J. Yang, "EMC experiment and protection method on control vehicle speed and distance measuring equipment of CRH2 HST," *Railway Signaling Commun. Eng.*, vol. 7, no. 5, pp. 21-24, Oct. 2010.
[11] J. P. Zhao and J. J. Gong, "Fault analysis and treatment of CRH2037A EMU's LKJ system," *Science & Technology Information*, no. 22, pp. 743-745, 2011.
[12] Y Guan, G Yue, W Chen, Z Li, and W Liu, "Experimental research on suppressing VFTO in GIS by magnetic rings," *IEEE Transactions on Power Delivery*, vol. 28, no. 4, pp. 2558-2565, Oct. 2013.
[13] M. Szewczyk, J. Pawlowski, K. Kutorasinski, and W. Piasecki, "High frequency model of magnetic rings for simulation of VFTO damping in gas-insulated switchgear with full-scale validation," *IEEE Transactions on Power Delivery*, vol. 30, no. 5, pp. 2331-2338, Oct. 2015.
[14] Z. T. Xiang, W. D. Liu, J. L. Qian, Y. L. Zhang, Y. Z. Shen, and S. P. Wang, "Simulation test and computation of suppressing very fast transient over-voltage in GIS by magnetic rings," *Proceedings of the Chinese Society for Electrical Engineering*, vol. 25, no. 19, pp. 101-105, Oct. 2005.
[15] Z. J. Shen. "Electromagnetic Interference Caused by Arc in Pantograph-Catenary System," *Department of Electrical Engineering, Beijing Jiaotong University, M.S.*, 2013.
[16] R. Tiedemann, "Current flow in coaxial braided cable shields," *IEEE Transactions on Electromagnetic Compatibility*, vol. 45, no. 3, pp. 531-537, Aug. 2003.
[17] P. M. Yang, T. B. Lu, L. Qi, and X. S. Gu, "Calculation of transfer impedance of braided shielded cable," *in Proceedings of The Symposium on Electrical Theory and New Technology*, Xi'an, China, pp. 318-321, Aug. 2005.
[18] R. Otin, J. Verpoorte, and H. Schippers, "Finite element model for the computation of the transfer impedance of cable shields," *IEEE Trans. On EMC*, vol. 54, no. 4, pp. 950-958, Nov. 2011.
[19] A. Morriello, T. M. Benson, A. P. Duffy, and C. F. Cheng, "Surface transfer impedance measurement: a comparison between current probe and pull-on braid methods for coaxial cables," *IEEE Trans. On EMC*, vol. 40, no. 1, pp. 69-76, Feb. 1998.
[20] S. Sali, "An improved model for the transfer impedance calculations of braided coaxial cables," *IEEE Trans. On EMC*, vol. 33, no. 2, pp. 139-143, May 1991.
[21] A. K. Bhattacharyya, *EMC Analysis Methods and Computational Models*, [M]. Wiley, 1997.
[22] Z. G. Yu, M. S. Liu, T. T. Zhang, W. F. Wei, G. Q. Gao, G. G. Wu, and B. C. Jia, "Test research on arcing during pantograph rising and lowering process for electric multiple units," *Electrical & Energy Management Technology*, no. 17, pp. 15-20, Sept. 2017.
[23] H. Zhang, Z. B. Zhao, and L. Liu, "Test research on the suppressing radio interference of DC transmission lines by ferrite cores," *Transactions of China Electrotechnical Society*, vol. 28, sup. 2, pp. 180-184, Dec. 2013.

Yutao Tang was born in Sichuan Province, China, in 1991. She received the B.S. degree in Automation from Southwest Science and Technology University, Mianyang, China, in 2013, and is currently working toward the Ph.D. degree in Electrical Engineering at Southwest Jiaotong University, Chengdu, China.

She has participated in the 2017 International Applied Computational Electromagnetics Society Symposium in China (ACES-China 2017) and made a presentation.

Her research interests include electromagnetic environment test and evaluation, and electromagnetic compatibility analysis and design.

Feng Zhu was born in Anhui Province, China, in 1963. He received the B.S. degree in Physics from Huaibei Normal University, Huaibei, China, in 1984, the M.S. degree in Physics from Sichuan University, Chengdu, China, in 1987, and the Ph.D. degree in Electro-

magnetic Theory and Microwave Techniques from Southwest Jiaotong University, Chengdu, in 1997.

He is currently a Professor in the Department of Electrical Engineering, Southwest Jiaotong University. His research interests include electromagnetic environment test and evaluation, electromagnetic compatibility, and numerical electromagnetic methods.

Hede Lu was born in Shandong Province, China, on October 4, 1988. He received the B.S. degree in Electronic Information Science and Technology from Southwest Jiaotong University, Chengdu, China, in 2012, and is currently working toward the Ph.D. degree.

His research interests include electromagnetic compatibility, electromagnetic environment test and evaluation, and transmission line analysis.

Xin Li received the B.S. degree in Electronic Information Science and Technology from Southwest Jiaotong University, Chengdu, China, in 2013. He is currently pursuing the Ph.D. degree in Electrical Engineering from Southwest Jiaotong University, Chengdu, China. His current research interests include analysis on the electromagnetic compatibility of electric locomotive.